Odovtos-International Journal of Dental Sciences (Odovtos-Int. J. Dent. Sc.), 27 (1): 73-85 (January-April), 2025. ISSN: 2215-3411
https://doi.org/10.15517/ijds.2024.62008

ODOVTOS
International Journal of Dental Sciences

UNIVERSIDAD DE COSTA RICA FOd Facultad de Odontología

https://revistas.ucr.ac.cr/index.php/Odontos

BASIC RESEARCH:

Effect of Epigenetic Inhibitors on Adipogenesis in Human Periodontal Ligament Stem Cells

Efecto de inhibidores epigéneticos en la adipogénesis en células troncales del ligamento periodontal humano

Julio A. Montero-Del-Toro[1-2] https://orcid.org/0009-0000-2745-3059
Angelica A. Serralta-Interian[1-2] https://orcid.org/0000-0003-2062-2141
Geovanny I. Nic-Can[2-3] https://orcid.org/0000-0001-8003-7716
Rafael Rojas-Herrera[1] https://orcid.org/0000-0001-8551-2336
Leydi M. Carrillo-Cocom[1] https://orcid.org/0000-0002-5477-7603
Beatriz A. Rodas-Junco[2-3] https://orcid.org/0000-0002-2804-6073

[1]Facultad de Ingeniería Química, Universidad Autónoma de Yucatán. Periférico Norte Kilómetro 33.5 Tablaje Catastral 13615 Chuburná de Hidalgo Inn. Mérida, Yucatán, CP 97203.
[2]Laboratorio de Células Troncales. Facultad de Odontología, Universidad Autónoma de Yucatán, calle 61A x 90 y 92. Mérida, Yucatán, C.P. 97000.
[3]CONAHCYT- Facultad de Ingeniería Química, Universidad Autónoma de Yucatán. Periférico Norte Kilómetro 33.5 Tablaje Catastral 13615 Chuburná de Hidalgo Inn, Mérida, Yucatán, C.P. 97203

Correspondence to: PhD. Beatriz A. Rodas-Junco - beatriz.rodas@correo.uady.mx

Received: 12-VI-2024 Accepted: 12-IX-2024

ABSTRACT: Histone H3 lysine 9 acetylation is a crucial epigenetic mark in mesenchymal stem cell differentiation processes like adipogenesis. This study aimed to evaluate the effect of epigenetic inhibitors on adipogenesis in human periodontal ligament stem cells, using histone deacetylase inhibitors such as valproic acid and trichostatin A. The cells were treated independently with 8 mM valproic acid and 100 nM trichostatin A for 72 hours to inhibit class I histone deacetylases. Subsequently, the cells underwent adipogenic induction for 28 days. Morphology and intracellular lipid deposition were analyzed using Oil-Red oil staining. Protein extracts were prepared on days 0 and 28 to analyze histone H3 lysine 9 acetylation levels via Western blot. Our results demonstrated that cells treated with either VPA or TSA showed, on average, a 1.275-fold increase in lipid deposition during the adipogenic process, with no significant differences between the treatments compared to the control group. Further, by day 28, histone H3 lysine 9 acetylation levels were 1.43 times higher in cells treated with valproic acid and 2.52 times higher in those treated with trichostatin A.These findings suggest that the inhibitors could have differential effects on chromatin remodeling in different regions by increasing acetylation, contributing indistinctly to lipid deposition due to the greater expression of genes associated with the adipogenic phenotype.

Odovtos -Int J Dent Sc endoses to CC-BY-NC-SA 4.0.

KEYWORDS: Histone acetylation; Periodontal ligament; Stem cell; Valproic acid; Trichostatin A.

RESUMEN: La acetilación de la histona H3 lisina 9 es una marca epigenética crucial en procesos de diferenciación de células madre mesenquimales como la adipogénesis. El objetivo de este estudio fue evaluar el efecto de los inhibidores epigenéticos sobre la adipogénesis en células madre humanas del ligamento periodontal, utilizando inhibidores de la histona desacetilasas como el ácido valproico y la tricostatina A. Las células se trataron independientemente con ácido valproico 8 mM y tricostatina A 100 nM durante 72 horas para inhibir las histonas desacetilasas de clase I. Posteriormente, las células se sometieron a inducción adipogénica durante 28 días. La morfología y la deposición intracelular de lípidos se analizaron mediante tinción con aceite Oil-Red. Se prepararon extractos de proteínas en los días 0 y 28 para analizar los niveles de acetilación de la histona H3 lisina 9 mediante Western blot. Nuestros resultados demostraron que las células tratadas con VPA o TSA mostraron, en promedio, un aumento de 1,275 veces en la deposición de lípidos durante el proceso adipogénico, sin diferencias significativas entre los tratamientos en comparación con el grupo control. Además, en el día 28, los niveles de acetilación de la histona H3 lisina 9 eran 1,43 veces superiores en las células tratadas con ácido valproico y 2,52 veces superiores en las tratadas con tricostatina A. Estos resultados sugieren que los inhibidores podrían tener efectos diferenciales sobre la remodelación de la cromatina en distintas regiones al aumentar la acetilación, contribuyendo indistintamente a la deposición de lípidos debido a una mayor expresión de genes asociados al fenotipo adipogénico.

PALABRAS CLAVE: Acetilación de histonas; Ligamento periodontal; Células troncales; Ácido valproico; Tricostatina A.

INTRODUCTION

Currently, obesity is a serious global health problem characterized by excessive development of adipose tissue. Adipose cells store energy from food in the form of triglycerides or fats (1). However, disruptions in this process can lead to greater fat accumulation and increased insulin resistance, potentially resulting in obesity and type II diabetes, among other metabolic diseases (2). The rising incidence of these issues has underscored the importance of studying the adipogenic process, for which mesenchymal stem cells (MSCs) serve as an excellent model. MSCs are undifferentiated cells capable of specializing in different lineages and have been identified in various human tissues. MSCs of dental origin have gained significant relevance due to their easy accessibility and minimal ethical limitations (2, 3).

The differentiation of stem cells, besides the molecular mechanisms of gene expression, is regulated by epigenetic factors (4, 5). Epigenetic regulation encompasses hereditary information that is not part of the genetic code but can influence gene expression. DNA is coiled around multiple histone units, forming an octamer of four different proteins known as histones (H2A/2B/3/4), which constitute chromatin in a dynamic structure that can become denser (heterochromatin) or more relaxed (euchromatin). Chromatin can modify its conformation through histone modifications like acetylation (6).

Histone acetylation is regulated by two main types of enzymes: histone acetylases (HATs) and histone deacetylases (HDACs). HATs catalyze the transfer of an acetyl group to the lysine (K) residues of histone tails. The negative charge of

the acetyl groups weakens the binding of nucleosomes to DNA, favoring chromatin relaxation and greater accessibility of certain genome regions for gene transcription. Conversely, HDACs promote the opposite effect by removing acetyl groups, favoring chromatin compaction, and restricting gene transcription (7). HDACs comprise up to 18 different enzymes distributed across seven families. Specifically, class I and II HDACs regulate histone acetylation within the nucleus (8). Epigenetic marks like histone H3 lysine 9 (H3K9ac) have been associated with cellular differentiation processes (9). HDAC inhibition is a strategy that can promote the transcription of genes of interest in cells subjected to stimuli like adipogenesis. Several HDAC inhibitors (iHDACs) have been reported in the literature, including suberoylanilide hydroxamic acid (SAHA), sodium butyrate (SB), valproic acid (VPA), and trichostatin A (TSA), inter alia (7).

HDAC inhibitors (iHDACs) such as VPA and TSA have been widely studied for their therapeutic applications. VPA, used clinically to treat epilepsy and bipolar disorders, acts primarily on class I and IIa HDACs, modulating gene expression through the inhibition of histone deacetylation. TSA, known for its selectivity towards class I HDACs, is being investigated for its potential in treating neurodegenerative diseases such as Alzheimer's and Parkinson's (10, 11). Both inhibitors stand out for their specific mechanisms and effects on epigenetic regulation, making them valuable tools for research into the development of new cellular therapies.

Regarding their mechanisms of action, VPA mainly inhibits HDACs of classes I and IIa by interfering with the catalytic site and chelating the zinc ion, resulting in the accumulation of acetylated lysine residues in histones and non-histone proteins, which modulates gene expression and promotes cell differentiation and apoptosis. TSA, particularly its (S)-TSA enantiomer, shows high selectivity toward HDAC6. TSA binds to the binding pocket of HDAC6 and chelates the zinc ion in the active site. However, the chirality of TSA and specific interactions within the binding pocket are critical for its selectivity toward HDAC6, thereby modulating protein acetylation more specifically than VPA (10, 11).

VPA and TSA in stem cell models of dental origin have been shown to positively affect promoting osteogenic (12) and odontoblastic differentiation (13), improving the deposition of calcium deposits within cells. Studying the regulation of histone acetylation in adipogenesis in a human stem cell model could enhance our understanding of the mechanism of adipogenic differentiation in humans, particularly concerning the role of this process in generating adipose tissue in conditions such as obesity. Therefore, this study aimed to analyze the effect of VPA and TSA on the adipogenesis of human periodontal ligament stem cells (PLSCs).

MATERIALS AND METHODS

Obtaining the biological material for this study was done according to the guidelines of the Research Ethics Committee of the "Dr. Hideyo Noguchi" Regional Research Center of the Autonomous University of Yucatán (UADY) (approval key: CIE-06-2017).

REACTIVATION AND CULTURE OF CELLS DERIVED FROM THE PERIODONTAL LIGAMENT

The PLSCs were obtained from the cell bank of the Translational Laboratory of Stem Cells of the Oral Cavity of the UADY, donated by a 17-year-old male patient with prior informed consent. The cells were reactivated under aseptic conditions and seeded in T25 culture dishes (Nest®), maintained with basal medium α-MEM (Minimum Essential Medium, Gibco) complemented by 15% fetal bovine serum (FBS, Gibco), and 1% antibiotic/antimycotic (penicillin [100 IU/mL] / streptomycin [100 µg/mL], Gibco). Finally, the cells were incuba-

ted under standard culture conditions of 37°C and 5% CO_2, with medium changes every 48 hours.

MULTILINEAGE CHARACTERIZATION

To evaluate the multipotent differentiation capacity of PLSCs at cell passage 6 (P6), cell differentiation assays toward chondrogenic, osteogenic, and adipogenic lineages were performed, as described by the International Society for Cellular Therapy (ISCT). The cells in P6 were recovered from the culture dishes by trypsinization, and 1×10^4 cells/well maintained with the basal medium were inoculated under standard conditions. When the cells reached 80% confluency, the culture medium in each plate was replaced with the specific induction medium for each lineage, using the StemPro™ chondrogenic differentiation Kit (Gibco™, A1007101) for 14 days, the StemPro™ osteogenic differentiation Kit (Gibco™, A1007201) for 14 days, and the StemPro™ adipogenic differentiation kit (Gibco™, A1007001) for 21 days. Cells cultured in α-MEM basal growth medium were used as an induction control. At the end of the cell differentiation assays, the cultures were stained using alcian blue (Sigma-Aldrich®) for chondrogenic nodules, alizarin red (Sigma-Aldrich®) for calcium deposits in osteogenesis, and Oil-Red oil (Sigma-Aldrich®) for staining lipid droplets in adipogenesis.

ANALYSIS OF PLURIPOTENCY AND MESENCHYMAL SURFACE MARKERS

To determine the differentiation capacity of PLSCs, the expression of embryonic stem cell markers was determined by PCR (*NANOG, SOX2, OCT4, KLF4, c-MYC*), and constitutive gene *18s*, and the markers for MSCs, both positive (CD73, CD90, and CD105) and negative (CD34 and CD45), by flow cytometry.

PCR analysis was performed from total RNA extracts from cell cultures at P6 using the RNA-Direct-zol kit (Zymo Research). For cDNA synthesis, reverse transcription reactions were performed with 1 µg of total RNA using the PrimeScript RT-PCR Kit (Takara Biotechnology, Dalian, China) following the manufacturer's instructions. The PCR reaction conditions were an amplification cycle of 40 seconds at 95°C, 30 seconds at the annealing temperature for each marker (Table 1), and 40 seconds at 72°C. PCR products were visualized on a 1.5% agarose gel (BIORAD) stained with SYBR GOLD.

Table 1. Sequence of primers for polymerase chain reaction (PCR) analysis.

Primers	Sequences	Sizes (pb)	Alignment Temperature (°C)
SOX2	F: 5′-ACA CCA ATC CCA TCC ACA CT-3′ R: 5′-CCT CCC CAG GTT TTC TCT GT-3′	120	62
NANOG	F: 5′-TGC TGA GAT GCC TCA CAC GGA-3′ R: 5′-TGA CCG GGA CCT TGT CTT CCT T-3′	120	60
OCT4	F: 5′-TGAA AGG GAC CGA GGA GTA-3′ R: 5′-CCG AGT GTG GTT CTG TAA C-3′	196	62
KLF4	F: 5′-TAC CAA GAG CTC ATG CCA CC-3′ R: 5′-CGC CTA ATC ACA AGT GTG GG-3′	114	60
c-MYC	F: 5′-GGA CCC GCT TCT CTG AAA GG-3′ R: 5′-TAA CGT TGA GGG GCA TCG TC-3′	104	60
18s	F: 5′-GGA CAG GAT TGA CAG ATT GAT-3′ R: 5′- AGT CTC GTT CGT TAT CGG AAT-3′	188	60

EFFECTS OF VALPROIC ACID AND TRICHOSTATIN A ON CELL MORPHOLOGY

To evaluate whether the inhibitors have negative effects on cell morphology, the cells were subjected to treatment with VPA and TSA for 72 hours. For this, the cells were seeded in 35 mm Petri dishes (Nest®) inoculating 1×10^4 cells. When the cells reached 50% confluency, the culture medium was supplemented in separate trials with 8 mM VPA or 100 nM TSA. Cells were also maintained with basal medium without inhibitors as a control. After 72 hours, the cells were washed with a 1X phosphate-buffered saline (PBS) solution adjusted to a pH of 7.4 and stained with 0.5% (w/v) crystal violet. Finally, morphology was evaluated with an inverted microscope (Leica, LM 2500).

ADIPOGENIC INDUCTION UNDER THE EFFECT OF VALPROIC ACID AND TRICHOSTATIN A

The PLCs at P6 were sown in T25 culture dishes by inoculating 3.5×10^4 cells maintained with basal culture medium under standard conditions. When the cells reached 80% confluency, the cultures were divided into different groups: cells with culture medium supplemented with 8 mM VPA, 100 nM TSA, and without inhibitors, for 72 hours. After three days of treatment, the culture medium of all groups was replaced by adipogenic induction medium (AIM), constituting day zero of induction. The AIM was changed thrice a week until 28 days of induction, and morphological changes were monitored with an inverted microscope (TCM 400, LABOMED).

LIPID DEPOSITION ANALYSIS

To determine the presence of intracellular lipids due to the adipogenic differentiation process, the culture dishes were washed with 1X PBS on day 28 of induction, and the cells were fixed with a 10% (w/v) paraformaldehyde solution for 10 minutes. Thereafter, the cells were washed with 60% isopropanol and allowed to dry for 3 minutes. Then the cells were stained using a 0.5% Oily-red O/60% isopropanol solution for 30 minutes at room temperature, followed by three washes with distilled water. The dye from the lipid droplets was then removed using 60% isopropanol, and absorbance was measured at 520 nm (Thermo, GENESYS 10 UV).

WESTERN BLOT ASSAY

Histone H3K9 acetylation changes due to adipogenic induction were evaluated using protein extracts from PLCs at days 0 and 28 of induction. Cells were collected via trypsinization, suspended in RIPA buffer with protease inhibitor, and sonicated for 60 seconds (CV18, Cole Parmer) with an amplitude of 50%. Protein concentration was determined using the bicinchoninic acid method.

For the Western blot assay, a concentration of 10 µg of the total extract was used to separate proteins by 10% SDS-PAGE electrophoresis. Subsequently, the proteins were transferred to a polyvinylidene fluoride (PVDF) membrane in Towbin running buffer (25 mM Tris-HCl, pH 8.3, 190 mM glycine, 20% v/v methanol) at 400 mA for 60 minutes. The PVDF membrane was then blocked with a solution of 1X PBS supplemented with 0.5% v/v Tween 20 (PBS-T) and 5% w/v Svelty® skim milk.

The H3K9ac protein was detected using a rabbit anti-H3K9ac monoclonal antibody (Invitrogen, 49-1009), while total histone H3 was identified with the rabbit anti-H3 monoclonal antibody (Invitrogen, PA5-119195) at dilutions of 1:2000 and 1:10,000, respectively. Both primary antibodies were incubated overnight at 4°C with constant stirring. As the secondary antibody, HRP-conjugated rabbit anti-goat IgG (Invitrogen, 31460) was used at a dilution of 1:20,000.

Finally, membranes were washed with PBS-T before incubating with the chemiluminescence

substrate (Millipore, Immobilon Western) according to the manufacturer's instructions. H3K9 acetylation levels were quantified relative to histone H3, using densitometry with ImageJ v.1.52 software.

STATISTICAL ANALYSIS

Each experiment consisted of three biological replicates. Statistical significance was determined using the ANOVA test with a Tukey post hoc test ($P<0.05$).

RESULTS

BIOLOGICAL CHARACTERIZATION

In differentiation assays, PLSCs exhibited the ability to differentiate toward chondrogenic, osteogenic, and adipogenic lineages, according to SITC criteria (Figure 1). Chondrogenesis showed elongated morphology (Figure 1.B) and changes in growth patterns compared to non-induced cells (Figure 1.A). Osteogenic differentiation demonstrated intracellular calcium deposits and culture surface mineralization via staining (Figure 1.C). Adipogenesis resulted in the formation of small lipid droplets (Figure 1.D). For pluripotency markers, *SOX2, NANOG, OCT4*, and *KLF4, c-MYC* were expressed positively (Figure 1.E), along with CD73, CD90, and CD105 mesenchymal phenotype markers (Figure 1.F). Additionally, negative markers ruled out heterogeneous cell populations of other types.

EFFECT OF EPIGENETIC INHIBITORS ON CELL MORPHOLOGY

The PLSCs cell population was treated with histone deacetylase inhibitors VPA (8 mM) and TSA (100 nM) for 72 hours to evaluate their impact on morphology and viability. After treatment, cells displayed an intact morphology, spindle-shaped or fibroblastoid, with no apparent damage. Cells treated with VPA showed a more flattened morphology and reduced cell confluency, compared to those treated with TSA (Figure 2.A and Figure 2.C).

EFFECT OF EPIGENETIC INHIBITORS ON ADIPOGENIC DIFFERENTIATION

Adipogenic differentiation was evaluated with the cells under pretreatment with VPA or TSA to determine how the inhibitors impact the cells maintained with the adipogenic induction medium. At day 0 of induction, pretreatment exposure with inhibitors did not cause any negative effects on cell morphology (Figure 3.A, Figure 3.B, Figure 3.C). Following 28 days of adipogenic differentiation, significant morphological changes were observed. Intracellular lipid droplets were formed both in the cells treated with AIM (Figure 3.D, Figure 3.E, Figure 3.F) and in those induced with VPA (AIM+VPA; Figure 3.G), as well as TSA (AIM+TSA; Figures 3.H). No notable differences in morphology were found between AIM+VPA cells (Figure 3.G) and AIM cells (Figure 3.F). However, smaller lipid droplets were observed within AIM+TSA-treated cells, compared to the other conditions.

INTRACELLULAR LIPID DEPOSITION

To quantify the impact of treatments on PLSCs differentiation capacity, intracellular lipid deposition was analyzed using Oily-Red O staining. A higher density of preadipocytes formed on the culture surface was observed in AIM+VPA (Figure 4.B) and AIM+TSA (Figure 4.C) cells, compared to AIM-treated cells (Figure 4.A).

The validity of these observations was supported by quantifying the amount of dye bound to lipids on culture surfaces through absorbance analysis. Compared to AIM-treated cells, AIM+VPA cells demonstrated a 1.27-fold increase in stained surface area, while AIM+TSA cells showed a minor discrepancy vis-a-vis AIM+VPA cells, with an increase of 1.28 times in the stained surface area relative to the control group.

TEMPORAL ACETYLATION PROFILE IN ADIPOGENESIS

To corroborate that the morphological and lipid deposition differences observed are due to HDACs inhibition, H3K9ac was analyzed by Western blot in cells with and without adipogenic induction. In cells maintained solely with basal culture medium (α-MEM), histone H3 was detected in cells treated with TSA (α-MEM+TSA) (Figure 5.A), but not H3K9ac (Figure 5.B). By day 28, an increase in acetylation levels was observed for each treatment, compared to day 0. Basal α-MEM cells showed a 2.18-fold higher level of acetylation (1.38 ± 0.09), while α-MEM +VPA cells exhibited no increase. On the other hand, in α-MEM +TSA cells (1.18 ± 0.15), H3K9ac was detected at levels similar to the control.

In adipogenic-induced cells (Figure 5), acetylation levels in control cells at day 0 were 1.57 times higher than in AIM+VPA cells and 1.12 times higher than in AIM+TSA cells (Figure 5.D). In AIM+TSA cells, a 1.55-fold increase in acetylation levels was observed on day 28, compared to day 0. A similar trend was observed in AIM+VPA cells, with a 1.1-fold increase in H3K9ac levels. These findings suggest that HDAC inhibition plays a role in the differentiation and lipid deposition process in adipocytes.

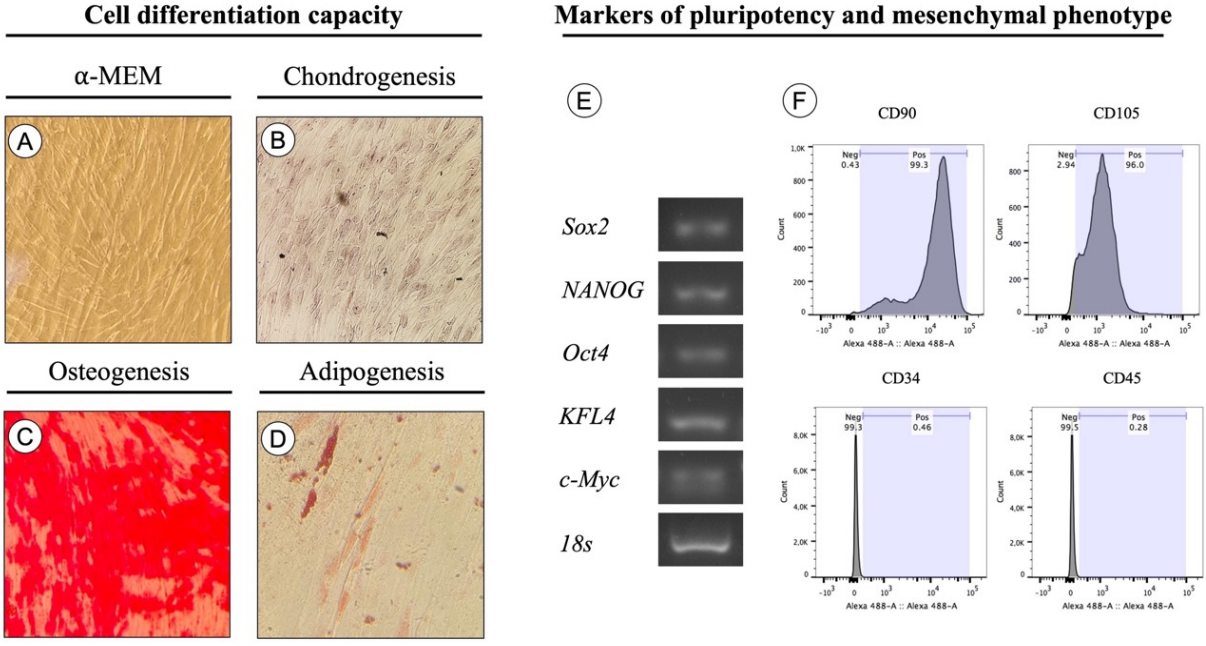

Figure 1. Biological characterization. (A-B) 20X microphotographs of cell differentiation assays. (A) Cells without induction of cell differentiation. (B) Cells after 14 days of chondrogenic induction stained alcian blue. (C) Cells after 14 days of osteogenic induction stained with alizarin red. (D) Cells after 21 days of adipogenic induction stained with oily red oil. (E) Flow cytometry of clusters of differentiation (CD) positive/negative from the mesenchymal. (F) Visualization of PCR products of mesenchymal surface markers.

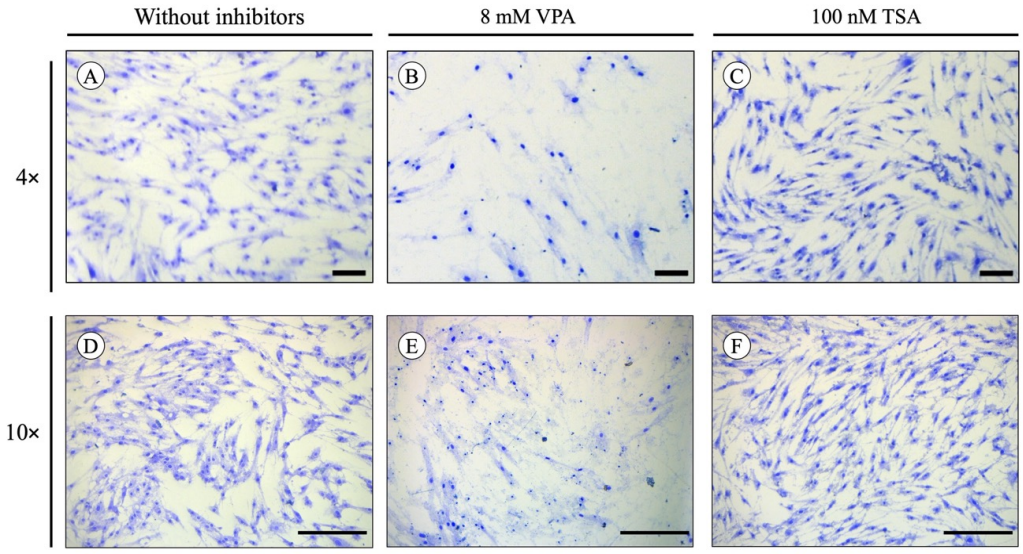

Figure 2. Morphological evaluation of the effect of epigenetic inhibitors. To visualize cell morphology, cells were stained with 0.5% (w/v) crystal violet after 72 hours of exposure. (A) Untreated cells. (B) Cells treated with valproic acid (VPA). (C) Cells treated with trichostatin A (TSA). Bar length = 500 µm.

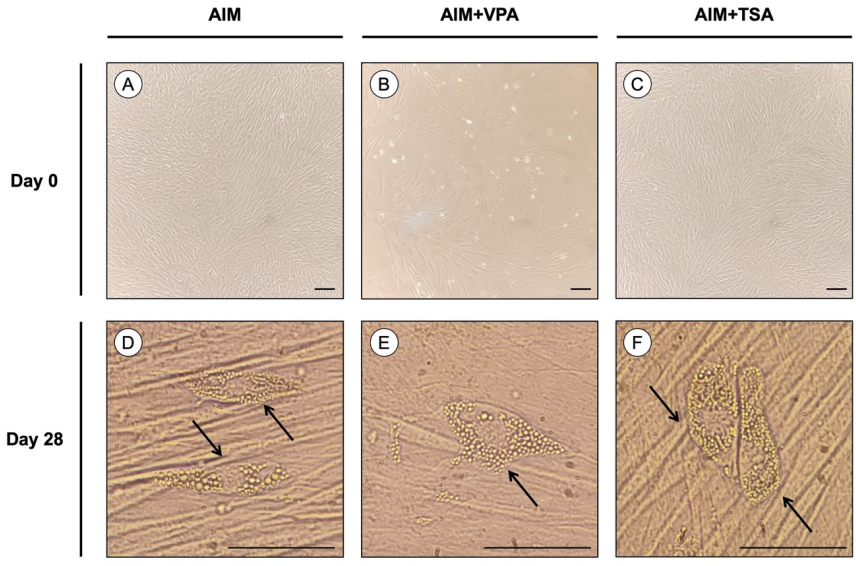

Figure 3. Adipogenic induction under the effect of the inhibitors valproic acid and trichostatin A. (A-C) 10X microphotographs of day zero with length bar = 50 µm (E-H). (D-F)20X microphotographs of day 28 with length bar = 50 µm. Cells with adipogenic induction medium (AIM) are not treated with inhibitors, the cells with 8 mM valproic acid (AIM+VPA) and 100 nM trichostatin A (AIM+TSA) were treated 72 h before induction.

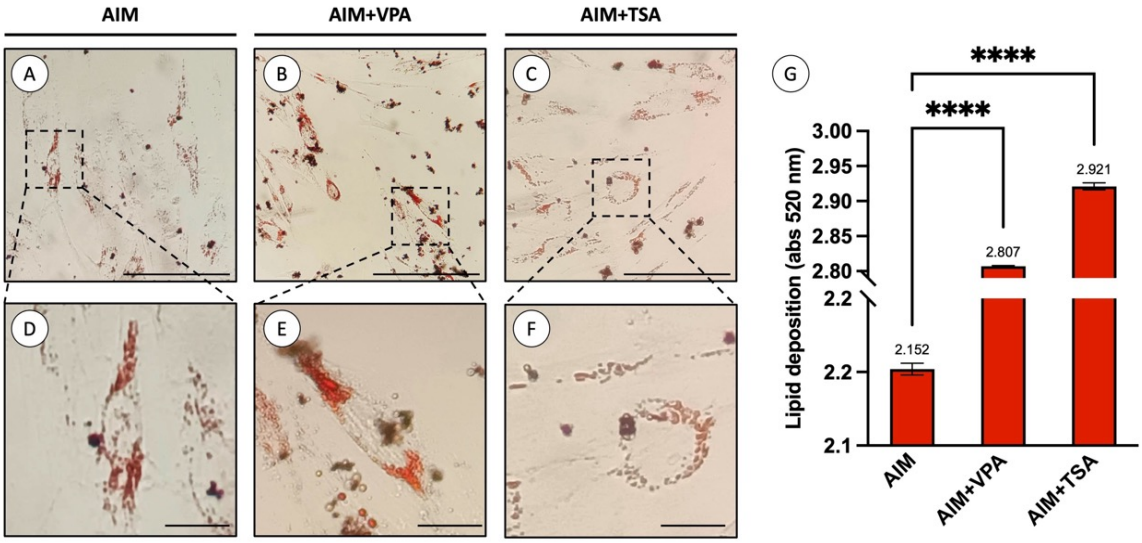

Figure 4. Evaluation of lipid deposition. Staining with oily red oil after 28 days of cells with adipogenic induction medium (AIM), without inhibitors, and cells with AIM under pretreatment with 8 mM valproic acid (AIM+VPA) and 100 nM trichostatin A (AIM+TSA). (A-C) Microphotographs at 10X, Length bar = 100 µm (D-F) Microphotographs at 20X, Length bar = 20 µm. (G) Graph of lipid deposition. The presence of the lipid-specific dye was determined by measuring the retention of the lipid-bound dye in the cultures by spectrometry at 520 nm. (n=3).

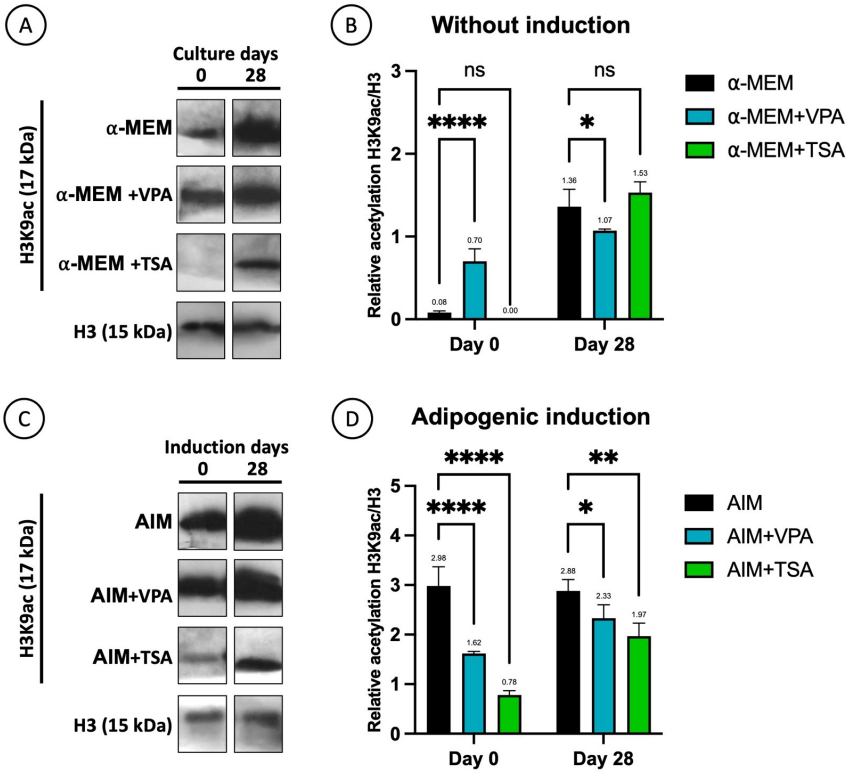

Figure 5. Acetylation profile of periodontal ligament stem cells. A) Western blot of histone H3K9ac and H3 in response to pretreatment of 8 mM valproic acid (VPA) and 100 nM trichostatin A (TSA) for 72 h on days zero and 28 of culture without induction of differentiation (loading 10 µg of protein). (B) Quantification of H3K9ac levels relative to H3 without the stimulation of cell differentiation. (C) Western blot of histone H3K9ac and H3 in response to pretreatment with inhibitors and adipogenic induction. (D) Quantification of H3K9ac levels to H3 under adipogenic differentiation. Densitometric analysis was performed with ImageJ software. Results are presented as mean ± standard deviation (n=3).

DISCUSSION

To evaluate the effect of class I HDAC inhibitors (VPA and TSA) on PLSCs, we aimed to better understand how these inhibitors influence PLSCs integrity, chromatin remodeling, and lipid deposition during adipogenesis.

MORPHOLOGICAL CHANGES INDUCED BY INHIBITORS

In the analysis of cell morphology using crystal violet staining, a notably lower confluency of PLSCs was observed after 72 hours of treatment with VPA (Figure 2.B). No differences were observed in the integrity or proliferation capacity of cells treated with TSA (Figure 2.C) and cells without inhibitors (Figure 2.A). This effect was mitigated throughout the study, reaching 28 days of cultivation (Figure 3.B). TSA treatment did not negatively impact cell proliferation capacity.

The influence of VPA in reducing growth capacity has been reported in other in vitro models, such as cells derived from human gingival tissue under the same concentration and exposure time 8 mM VPA for 72 hours (8). For human PLSCs, studies have shown that VPA at lower concentrations does not negatively affect cell proliferation over short periods, at 1.5 mM VPA (14). However, prolonged treatments have shown a reduction in proliferation capacity, at 1 mM VPA (12).

DEPOSITION OF LIPID DROPLETS DUE TO EPIGENETIC INHIBITORS

When evaluating the formation of intracellular lipid droplets, a characteristic phenotype of adipogenic differentiation, it was observed on day 28 of adipogenic differentiation that the lipid droplets formed by the AIM+TSA cells (Figure 4.C) were smaller, compared to the other groups (Figure 4.A, Figure 4.B). This suggests that the inhibitors have differential effects in modulating lipid metabolism. Analysis of lipid deposition by Oil Red O staining (Figure 4) showed that epigenetic inhibitors promoted greater lipid deposition in both AIM+VPA and AIM+TSA cells compared to the control (Figure 4.G). The differences in droplet size could indicate that the selectivity of the inhibitors modulates different regions of chromatin involved in the transcription of adipogenic markers.

Although there are no reports on the effects of these inhibitors on adipogenesis of cells from dental origin, their effects have been described in other cell models. Daily exposure to VPA (≥ 1 mM) and TSA (≥ 3 nM) in murine preadipocytes has been observed to lead to decreased lipid deposition, as analyzed by Oil Red O staining (15). In preadipocytes and human umbilical cord cells under adipogenic induction, treatment with VPA at concentrations of 1 and 10 mM every 24 hours resulted in reduced formation of intracellular lipid droplets and lower lipid detection by Oil Red O staining, compared to cells without the inhibitor (16).

The differences found in this study vis-a-vis the literature could be attributed to variations in cell types, culture conditions, and specific concentrations and exposure times of the inhibitors used.

Several factors, such as the cell model used or the origin of the cells, the specific cellular environment, differentiation potential, and responsiveness to inhibitors like VPA and TSA, may vary between different cell types.

LINKING H3K9AC ACETYLATION LEVELS TO ADIPOGENIC RESPONSE

When evaluating whether these changes are associated with the effect of inhibitors on enhancing acetylation in the H3K9 mark, western blot analysis showed that the cells without AIM treated with VPA exhibited a significant increase in H3K9ac levels on day zero, while no significant acetylation was detected in cells treated with TSA (Figure

5.C). The absence of H3K9ac in α-MEM+TSA cells could be associated with the undetectable levels of histone H3K9ac (Figure 5.B), suggesting that the effect on acetylation in H3K9 by TSA occurred later, compared to α-MEM and α-MEM+VPA cells.

However, global chromatin acetylation is a dynamic process occurring at different modification sites. Despite this, cells without AIM under treatment toward day 28 demonstrated increased acetylation levels with both inhibitors (Figure 5.C), indicating that both can potentially increase acetylation (Figure 5.A).

For cells maintained with AIM, acetylation levels were quite high on day zero in cells without inhibitors (Figure 5.F). This could be attributed to the adipogenic induction medium triggering chromatin remodeling response to promote cell differentiation (Figure 5.D). By day 28, treatments with VPA and TSA increased H3K9ac levels (Figure 5.C) and positively affected the differentiation capacity of PLSCs, leading to greater lipid deposition, compared to cells without inhibitors (Figure 4). This suggests that the inhibitors could affect the dynamics of acetylation, enhancing the transcription of adipogenic genes.

The positive effect of increasing acetylation on cellular plasticity has been reported in various models and studies. For example, in murine ESCs, TSA (5 or 25 nM) and VPA (0.5 mM) significantly increased H3K9ac levels (17). In human cells, HDAC inhibitors like VPA enhanced differentiation efficiency (VPA 0.1 or 0.5 mM), as in PDLSCs from human third molars (12). In human embryonic cells, TSA (10 ng/mL) increased H3K9ac levels, promoting neuronal genes while repressing pluripotency genes (18).

Although hyperacetylation generated by inhibitors seems to enhance lipid deposition, additional assays are needed to better understand the dynamics of H3K9 acetylation and its impact on adipogenic gene expression. Evaluating shorter or intermediate time points and performing expression analyses of the main adipogenic markers in future research would be advisable.

CONCLUSION

The histone deacetylase inhibitors VPA and TSA demonstrated the ability to promote adipogenic differentiation in PLSCs by increasing H3K9ac levels. VPA initially reduced cell confluency, whereas TSA preserved cell integrity, reflecting their distinct impacts on cell morphology. Both inhibitors also enhanced lipid droplet formation, indicating their role in modulating lipid metabolism during adipogenesis. To gain a comprehensive understanding of the mechanisms by which these inhibitors facilitate adipogenesis, future research should focus on the expression of key adipogenic genes and perform acetylation enrichment assays.

AUTHOR CONTRIBUTION STATEMENT

Conceptualization: B.A.R-J.
Writing-original draft preparation: J.A.M-D; A.A.S-I.
Methodology: G.I.N-C, J.A.M-D; A.A.S-I.
Data curation: J.A.M-D; A.A.S-I
Writing-review and editing: B.A.R-J; G.I.N-C, R.R-H, and L.M.C-C.

All authors have read and agreed to the published version of the manuscript.

CONFLICT OF INTEREST

The authors declare that they have no conflicts of interest.

ACKNOWLEDGEMENTS

This study was supported by Consejo Nacional de Humanidades, Ciencia y Tecnología (CONAHCYT) grants awarded to Beatriz A. Rodas-Junco (Ciencia de Frontera-429849) and postdoc-

toral fellowship for Angelica Serralta-Interian (No. 474112). The authors acknowledge the support of the Laboratorio de Celulas Troncales de la Facultad de Odontología de la Universidad Autónoma de Yucatán and the Seeding Labs program.

REFERENCES

1. González-Casanova J.E., Pertuz-Cruz S.L., Caicedo-Ortega N.H., Rojas-Gomez D.M. Adipogenesis Regulation and Endocrine Disruptors: Emerging Insights in Obesity. Vol. 2020, BioMed Research International. 2020.
2. Rodas-Junco B.A., Canul-Chan M., Rojas-Herrera R.A., De-la-Peña C., Nic-Can G.I. Stem cells from dental pulp: What epigenetics can do with your tooth. Front Physiol. 2017; 8: 899.
3. Rajabzadeh N., Fathi E., Farahzadi R. Stem cell-based regenerative medicine. Stem Cell Investig. 2019; 6 (July).
4. Ozkul Y., Galderisi U. The Impact of Epigenetics on Mesenchymal Stem Cell Biology. Vol. 231, Journal of Cellular Physiology. 2016. p. 2393-401.
5. Wu H., Yi E.S. Epigenetic regulation of stem cell differentiation. Vol. 59, Pediatric Research. 2006.
6. Shukla V., Vaissière T., Herceg Z. Histone acetylation and chromatin signature in stem cell identity and cancer. Vol. 637, Mutation Research - Fundamental and Molecular Mechanisms of Mutagenesis. 2008. p. 1-15.
7. Lawlor L., Yang X.B. Harnessing the HDAC-histone deacetylase enzymes, inhibitors and how these can be utilised in tissue engineering. Vol. 11, International Journal of Oral Science. 2019.
8. Lee H., Lee J.Y., Ha D.H., Jeong J.H., Park J.B. Effects of valproic acid on morphology, proliferation, and differentiation of mesenchymal stem cells derived from human gingival tissue. Implant Dent. 2018; 27 (1).
9. Jang S., Hwang J., Jeong H.S. The Role of Histone Acetylation in Mesenchymal Stem Cell Differentiation. Chonnam Med J. 2022; 58 (1).
10. Sixto-López Y., Bello M., Correa-Basurto J. Exploring the inhibitory activity of valproic acid against the HDAC family using an MMGBSA approach. J Comput Aided Mol Des. 2020; 34 (8).
11. Zhang Y., Ying J.B., Hong J.J., Li F.C., Fu T.T., Yang F.Y., et al. How Does Chirality Determine the Selective Inhibition of Histone Deacetylase 6? A Lesson from Trichostatin A

Enantiomers Based on Molecular Dynamics. ACS Chem Neurosci. 2019; 10 (5).
12. Um S., Lee H., Zhang Q., Kim H.Y., Lee J.H., Seo B.M. Valproic Acid Modulates the Multipotency in Periodontal Ligament Stem Cells via p53-Mediated Cell Cycle. Tissue Eng Regen Med. 2017; 14 (2).
13. Gu S., Liang J., Wang J., Liu B. Histone acetylation regulates osteodifferentiation of human dental pulp stem cells via DSPP. Front Biosci (Landmark Ed). 2013; 18.
14. La Noce M., Mele L., Laino L., Iolascon G., Pieretti G., Papaccio G., et al. Cytoplasmic interactions between the Glucocorticoid receptor and HDAC2 regulate Osteocalcin expression in VPA-Treated MSCs. Cells. 2019; 8 (3).
15. Catalioto R.M., Maggi C.A., Giuliani S. Chemically distinct HDAC inhibitors prevent adipose conversion of subcutaneous human white preadipocytes at an early stage of the differentiation program. Exp Cell Res. 2009; 315 (19).
16. Lee S., Park J.R., Seo M.S., Roh K.H., Park S.B., Hwang J.W., et al. Histone deacetylase inhibitors decrease proliferation potential and multilineage differentiation capability of human mesenchymal stem cells. Cell Prolif. 2009; 42 (6).
17. Hezroni H., Tzchori I., Davidi A., Mattout A., Biran A., Nissim-Rafinia M., et al. H3K9 histone acetylation predicts pluripotency and reprogramming capacity of ES cells. Nucleus. 2011; 2 (4): 300-9.
18. Qiao Y., Wang R., Yang X., Tang K., Jing N. Dual roles of histone H3 lysine 9 acetylation in human embryonic stem cell pluripotency and neural differentiation. Journal of Biological Chemistry. 2015; 290 (4): 2508-20.